

Human Placentas, Optimal Transportation and High-risk Autism Pregnancies

Qinglan Xia^{1,*}, Lisa A Croen², M. Danielle Fallin³, Craig J Newschaffer⁴, Cheryl Walker⁵, Philip Katzman⁶, Richard K Miller⁶, John Moye⁷, Simon Morgan⁸, and Carolyn M. Salafia⁹

¹*Department of Mathematics, University of California at Davis, One Shields Ave, Davis, CA, 95616*

²*Division of Research, Kaiser Permanente Northern California, Oakland, CA,*

³*Wendy Klag Center for Autism and Developmental Disabilities, Department of Mental Health, Johns Hopkins Bloomberg School of Public Health, Baltimore, MD,*

⁴*AJ Drexel Autism Institute, Drexel University, Philadelphia, PA,*

⁵*Department of Obstetrics and Gynecology, MIND Institute, University of California Davis, Sacramento, CA,*

⁶*University of Rochester Medical Center, Rochester, NY*

⁷*National Institute of Child Health and Human Development, Rockville, MD*

⁸*Department of Physics, Imperial College London and*

⁹*Placental Analytics, New Rochelle, NY.*

(Dated: Invited Paper 31/08/16, Accepted 05/09/16)

The aim of this article is to study the traced vascular structures inside (human) placentas via optimal transportation techniques from two groups of births - one from mothers who already have a child diagnosed with ASD and the other from a general-population birth cohort. Younger siblings of children diagnosed with ASD are themselves at several-fold greater risk of being diagnosed with ASD. Consequently, this comparison can provide an initial indication of whether placental vascularization might be deserving of further study in etiologic research on prenatal neurodevelopment and as a potential ASD risk biomarker. Our results show that vascular structures quantified by transport efficiency in placentas belonging to newborns at higher ASD risk are significantly different from those in placentas from the population-based control cohort.

Keywords: Optimal Transportation, Branching Structure, Transport Efficiency, Placenta, Autism, Shape Factor.

MSC: Primary 82B24, 49Q20; Secondary 28A80, 74P05.

1. INTRODUCTION

Autism spectrum disorder (ASD) is one of the fastest-growing developmental disabilities in the United States. People with ASD have impairment in social communication and interaction along with restricted and repetitive patterns of behaviors, interests or activities [1]. U.S. Centers for Disease Control and Prevention ASD surveillance reported ASD prevalence in 2012 among US 8 year olds to be 1 in 68 [6], more than two-fold greater than the CDC estimate of 1 in 150 reported a decade earlier [2].

ASD is diverse in its presentation; no two people with ASD will have exactly the same symptoms or manifestations. There is no medical cure for ASD, and it is often complicated and difficult to diagnose accurately. Nevertheless, ASD appears to have its roots in very early brain development. According to [7] [17], the earlier children with ASD are identified and receive evidence-supported intervention, the greater their chance of positive outcomes. Children with an ASD diagnosis who received early intervention tend to

have better outcomes, improved communication skills and enhanced overall social behavior compared to ASD children with no early intervention. Cost of lifelong care can be reduced by 2/3 with early diagnosis and intervention. However, the most obvious signs and symptoms of ASD tend to emerge between 2 and 3 years of age. Interest is intense in determining if there are any valid and reliable indicators of ASD risk measurable at earlier ages.

Here we conduct a comparison of the vascular networks of placentas collected from the births of siblings of older children diagnosed with ASD to the vascular networks of placentas from a general population sample of births. Siblings of children with an ASD diagnosis are at several-fold higher risk of themselves being diagnosed with an ASD [16], [19]. The placenta is a temporary organ that serves in the exchange of nutrients and wastes between the mother and the fetus. ASD appears to have its roots in fetal life, which is highly dependent on the dynamic growth function of the placenta. Information about the timing and possibly the nature of early brain maldevelopment may be paralleled by alterations in the geometric structure of the placenta as measured by its size, shape and depth, as well as by the thickness, length, and geometric locations of its veins and arteries. Related study of placentas can be found in the works of [27], [12], [10], [13],[28], [29] and references

*Corresponding author. Email: qlxia@math.ucdavis.edu. URL: <http://math.ucdavis.edu/~qlxia>

therein.

In a previous article [25], the authors quantified efficiency of the transport system in the human placenta and studied its correlation with birth weight and gestational age of newborns. In those data, each placenta was represented by a planar domain and a fixed point representing the site of the umbilical cord insertion. By means of techniques in ramified optimal transportation (see Section 2 for details), the authors simulated a vascular tree structure for the placenta in simplified form, by an idealized optimal transport network. The main result in [25] showed that averaged birth weight and averaged gestational age were both roughly increasing functions of the calculated placental transport efficiency. Both preterm birth and low birth weight were associated with lower placental transport efficiency. The authors also showed that the relationship of transport efficiency to these outcomes was nonlinear, reaching a plateau at 38 – 39 weeks gestational age and 3200g birth weight.

In [25], we only used the locations of the boundary curves of the placental chorionic surface and the umbilical cord insertion point. Recently, we have manually traced arterial (Figure 4) and venous vascular networks from the following two groups of placentas:

- NCS placentas: 201 placentas collected by the National Children’s Study (NCS) [14]. NCS is a population cohort study of children in the United States and as such would be expected to experience the baseline ASD risk seen in the general U.S. population.
- EARLI placentas: 75 placentas collected by the Early Autism Risk Longitudinal Investigation (EARLI) Study. The EARLI Study enrolled mothers of children with ASD at the start of another pregnancy and followed the development of the newborn child to age three [15]. Siblings of children with ASD have a several-fold higher risk of receiving an ASD diagnosis than do children in the general population [16], [19].

Our main result indicates that under suitable transportation cost, there is significant difference in transport efficiency of the measured venous/arterial networks between the NCS and the EARLI placentas, with EARLI placentas demonstrating both lower overall transport efficiency and lower ratios of venous vs. arterial network transport efficiency.

The article is organized as follows: We first recall some basic definition of ramified optimal transportation in section 2. Then, we recall the concepts of transport efficiency and shape factor of placentas in section 3. The main work is stated in section 4. We trace the geometry of the actual arterial and venous vasculatures on the planar chorionic surfaces from both NCS and EARLI placentas. Then, we compare transport efficiency of traced vascular networks in placentas of the EARLI group to those of the NCS group, with

respect to various transportation cost functions. The calculated transportation efficiency quantifies the difference between these two groups. We also compare these two groups of placentas with respect to a fixed transport cost function: the quadratic cost function.

2. BRIEF INTRODUCTION TO RAMIFIED OPTIMAL TRANSPORTATION

The optimal transportation problem aims at finding an optimal way to transport materials from the source to the target. An optimal transport path introduced in [20] is a mathematical concept used to model efficient branching transport networks. Transport networks with branching structures are observable not only in nature as in trees, blood vessels, river channel networks, lightning, etc. but also in efficiently designed transport systems such as used in railway configurations and postage delivery networks. Recently, mathematicians (e.g.: [20] [11][5][4]) have shown great interest in modeling these transport networks with branching structures. Applications of optimal transport paths may be found in e.g. [21] and [24]. A survey of this research field can be found in [26].

We first recall some basic concepts of ramified optimal transportation as stated in [20]. Recall that a (finite) atomic measure on the Euclidean space \mathbb{R}^m is in the form of

$$\mathbf{a} = \sum_{i=1}^k m_i \delta_{x_i} \quad (1)$$

with distinct points $x_i \in \mathbb{R}^m$, and positive real numbers m_i , where δ_x denotes the Dirac mass located at the point x .

Given two atomic measures

$$\mathbf{a} = \sum_{i=1}^k m_i \delta_{x_i} \text{ and } \mathbf{b} = \sum_{j=1}^{\ell} n_j \delta_{y_j} \quad (2)$$

in \mathbb{R}^m of equal mass (i.e. $\sum_{i=1}^k m_i = \sum_{j=1}^{\ell} n_j$), a **transport path** from \mathbf{a} to \mathbf{b} is a weighted directed graph G consisting of a vertex set $V(G)$, a directed edge set $E(G)$ and a weight function $w : E(G) \rightarrow (0, +\infty)$ such that $\{x_1, x_2, \dots, x_k\} \cup \{y_1, y_2, \dots, y_{\ell}\} \subset V(G)$ and for any vertex $v \in V(G)$,

$$\begin{aligned} & \sum_{e \in E(G), e^- = v} w(e) - \sum_{e \in E(G), e^+ = v} w(e) \\ &= \begin{cases} m_i, & \text{if } v = x_i \text{ for some } i = 1, \dots, k \\ -n_j, & \text{if } v = y_j \text{ for some } j = 1, \dots, \ell \\ 0, & \text{otherwise} \end{cases} \end{aligned}$$

where e^- and e^+ denotes the starting and ending endpoints of each edge $e \in E(G)$. Note that this balanced equation simply means the conservation of mass at each vertex.

Suppose \mathbf{a} and \mathbf{b} are two atomic measures on \mathbb{R}^m of equal total mass. For any real number $\alpha < 1$ and any transport path G from \mathbf{a} to \mathbf{b} , we define its *transport cost* to be

$$\mathbf{M}_\alpha(G) := \sum_{e \in E(G)} w(e)^\alpha \text{length}(e), \quad (3)$$

where $\text{length}(e)$ denotes the Euclidean distance between endpoints of the edge e .

Let $\text{Path}(a, b)$ be the space of all transport paths from \mathbf{a} to \mathbf{b} . A transport path G from \mathbf{a} to \mathbf{b} is called an α -*optimal transport path* if

$$\mathbf{M}_\alpha(G) \leq \mathbf{M}_\alpha(\tilde{G})$$

for any other transport path \tilde{G} from \mathbf{a} to \mathbf{b} . Also, the d_α distance between \mathbf{a} and \mathbf{b} is defined to be

$$d_\alpha(\mathbf{a}, \mathbf{b}) = \min \{ \mathbf{M}_\alpha(G) : G \in \text{Path}(\mathbf{a}, \mathbf{b}) \}. \quad (4)$$

In general, for any two Radon measures μ and ν on \mathbb{R}^m with equal mass, the d_α distance between μ and ν is given by

$$d_\alpha(\mu, \nu) = \lim_{n \rightarrow \infty} d_\alpha(\mathbf{a}_n, \mathbf{b}_n), \quad (5)$$

for any two sequence $\{\mathbf{a}_n\}, \{\mathbf{b}_n\}$ of atomic measures converge weakly to μ and ν , respectively.

Some numerical simulations of optimal transport paths were given in [23, 26]. Applications of optimal transport path may be found in e.g. [21], [24] and [22]. For instance, we have used the idea of this theory to describe the dynamic formation of a plant leaf in [21].

3. TRANSPORT EFFICIENCY OF THE HUMAN PLACENTA

The placenta is the sole source of fetal nutrients and oxygen. Placental transport function is critical to the health and development of the fetus. According to the fetal origin of adult health hypothesis [3], placental development continues to be linked to health in adulthood, beyond infancy and childhood. In [25], we introduced the concept “transport efficiency” of the placenta and studied its relationship with birth weight and gestational age. Since it is closely related to the methods in this article, we briefly recall its motivation and definitions here.

In previously published work [25], based on a sample of 1110 placentas collected by an academic health center in central North Carolina, we investigated the role that the shape of the placenta (including location of the umbilical cord) played in the birth weight of the newborn. Similar to what was done in this study, a trained observer took a photo of each placenta (Figure 1) and captured a series of x, y



FIG. 1: A photo of a placenta

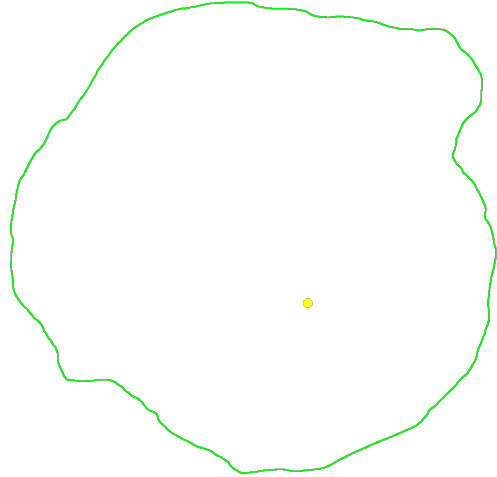


FIG. 2: Boundary curve and the umbilical cord insertion point of the placenta.

coordinates that marked the site of the umbilical cord insertion and the boundary curve of the fetal surface (Figure 2). When comparing those placentas, we wanted to remove the impact of the size and consider only the effect of shape. To do so, we introduced the variable “shape factor” as follows.

As stated above, each placenta P is represented by a pair (D, O) where D is a bounded domain in \mathbb{R}^2 and O is a fixed point inside D representing the site of the umbilical cord insertion. We say two placentas $P_1 = (D_1, O_1)$ and $P_2 = (D_2, O_2)$ have the same *shape* if they are similar to each other. In other words, there exists a number $\lambda > 0$ and a 2×2 orthogonal matrix A such that the mapping $f_\lambda : D_1 \rightarrow D_2$ given by

$$f_\lambda(x) = \lambda A(x - O_1) + O_2, x \in D_1$$

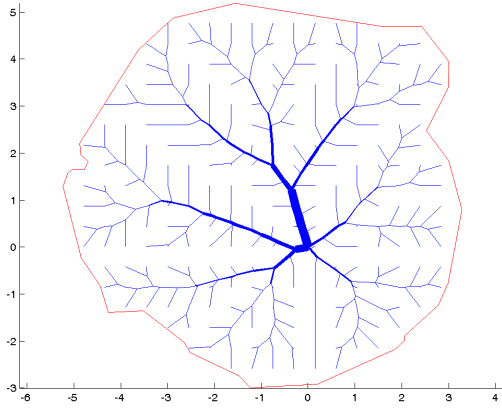


FIG. 3: An approximate optimal transport network modeling the vascular structure inside the placenta.

is one-to-one and onto.

For each placenta $P = (D, O)$ and $\alpha < 1$, the α -shape factor of P is defined by

$$S_\alpha(P) := \frac{d_\alpha(\mu_D, |D| \delta_O)}{|D|^{\alpha+0.5}},$$

where μ_D denotes the Lebesgue measure of \mathbb{R}^2 restricted on the set D , $|D|$ denotes the area of D , and d_α is the distance defined in (5). It turns out that two placentas of the same shape have the same shape factor S_α .

Since transportation cost $d_\alpha(\mu_D, |D| \delta_O)$ is proportional to the shape-factor S_α , among placentas of similar sizes, the smaller the shape-factor S_α the more efficient was the transport system corresponding to the placenta. This motivates us to consider the following definition. For each placenta P and $\alpha < 1$, the transport α -efficiency of P is defined to be

$$E_\alpha(P) := \frac{S_\alpha(B(0, 1))}{S_\alpha(P)},$$

where $S_\alpha(B(0, 1))$ denotes the α -shape factor of the unit ball $B(0, 1)$ in \mathbb{R}^2 with respect to the origin $(0, 0)$. Clearly, two placentas of the same shape have the same transport efficiency.

To calculate the transport cost $d_\alpha(\mu_D, |D| \delta_O)$, we used algorithms describe in [23, 26] to generate an approximated optimal transport path $G_P \in \text{Path}(\mu_D, |D| \delta_O)$. This leads to Figure 3. We used this idealized transport system G_P to model the vein (or the arterial) structure inside the placenta. The value $d_\alpha(\mu_D, |D| \delta_O)$ is approximated by $M_\alpha(G)$. Thus,

$$S_\alpha(P) \approx \frac{M_\alpha(G_P)}{|D|^{\alpha+0.5}}. \quad (6)$$

For each placenta P in the available data and $\alpha = 0.85$, we calculated the transport cost $M_\alpha(G_P)$, shape-factor $S_\alpha(P)$ as well as the transport efficiency $E_\alpha(P)$, and then studied their relations with the recorded data on birth weights and gestational ages. The following summarizes what we have found in [25].

- The average of transport cost $M_\alpha(G_P)$ for any given birth weight is nearly a linear function of the birth weight. Transport cost is positively correlated with birth weight as expected, given that it primarily reflects placental size, and on average will vary with larger and smaller placental and fetal weights.
- Averaged transport efficiency for any given birth weight is roughly an increasing function of the birth weight. The smaller the birth weight, the less efficient the placenta. This demonstrates that transport efficiency of the placenta is an important correlate of birth weight.
- Average birth weight for any fixed transport efficiency still increases as transport efficiency increases, but with a decreasing slope.
- Averaged transport efficiency is roughly an increasing function of gestational ages. Preterm newborns typically have less efficient placentas compared to infants born at term. This is consistent with the progressive development of vasculosyncytial membranes from the beginning of the third trimester [12].
- Average gestational age still increases as transport efficiency increases, but again with a decreasing slope.

Consequently, we previously showed that transport efficiency of a placenta as estimated from simple measures of perimeter and the location of umbilical cord insertion in the chorionic plate was highly correlated with birth weight and gestational age, and also that this relationship changed over gestational age and birth weight ranges consistent with what is well appreciated clinically [10].

Moreover, the calculated transport efficiency demonstrated transitions that allowed clear distinctions to be proposed between newborns exposed to an inefficient placenta (and hence to a compromised intrauterine environment) and those with adequate placental transport efficiency.

4. NEW PLACENTAL DATA AND NEW MEASUREMENTS

In this study we improved transport efficiency estimates by adding new measures of surface vasculature to measures of placenta boundary and umbilical cord position. All

EARLI and NCS placentas investigated here had a 2D digital photograph taken of the chorionic plate by a trained photographer, and both the vein and artery structures (see Figure 4) were traced from the photograph following methods described in [29] and [30]. Our interest here was to distinguish these two groups by studying their corresponding vascular networks via optimal transportation techniques.

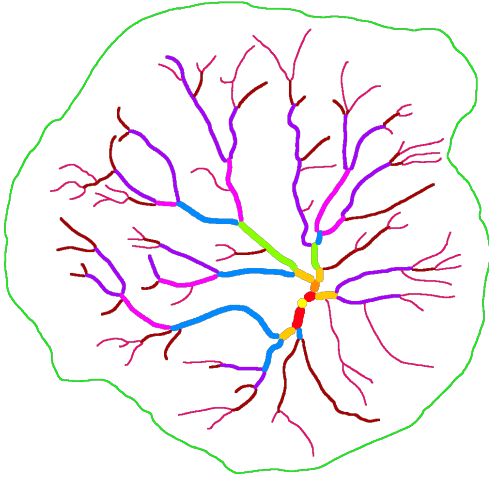


FIG. 4: Hand traced arterial vasculature

Remark: Here, for simplicity as well as accuracy, we used manually traced vein/arteries structures in our current study (colors and thicknesses are chosen by the tracer to indicate visible width of vessels). As described in [30], automated segmentation of the vessels from the images without tracings has not been successful because the vessels, after the placenta was cut off from the baby, deflated inconsistently. As a result, some segments were blood filled and dark while others were bloodless and appeared pale, causing a significant problem for applying automated image segmentation. On the other hand, if an alternative possibly more efficient way (e.g. some blood vessel segmentation methodologies [9]) could overcome these problems in the future, it is still expected that replacing manually traced vein/arteries structures by structures derived from a reasonable blood vessel segmentation methodology will not change essential results of our study.

Each traced arterial/venous vascular networks gives a weighted directed graph G . For each blood vessel segment e of length $l(e)$, let

$$f(w(e), l(e))$$

be the cost of transporting a volumetric flow rate $w(e)$ along the segment e . In particular, we are interested in the cost function of the form

$$f(x, y) = x^\alpha y^\beta$$

for real valued parameters α and β . The corresponding transportation cost of G is

$$M_{\alpha, \beta}(G) = \sum_{e \in E(G)} w(e)^\alpha l(e)^\beta,$$

where $E(G)$ is the set of all edges of G .

Remark: Here, our choice of selecting $f(x, y) = x^\alpha y^\beta$ is motivated by ramified optimal transportation theory. We hope to use this family of transportation cost functions as an example to find some measurable quantities that can distinguish the vascular networks inside the NCS and EARLI placentas. Nevertheless, it is reasonable to expect that some other family of transportation cost functions (e.g. the one used in [21]) might also be used for similar purpose.

A benchmark for vascular systems was proposed by Murray in 1926 as a compromise between the frictional and metabolic costs, with the latter expressed as a cost function. The formulation of a minimum energy hypothesis led to a scaling law, $w(e) \propto d(e)^3$, between the volumetric flow rate $w(e)$ and the diameter $d(e)$ of a blood vessel segment e . This scaling law is universal for all trees whose internal flows are laminar. By Murray's law, it holds that

$$M_{\alpha, \beta}(G) \propto \sum_{e \in E(G)} d(e)^{3\alpha} l(e)^\beta. \quad (7)$$

Motivated by (6), we use a normalization process to remove the effect of the size of the placenta on $M_{\alpha, \beta}(G)$. When one rescales the planar domain D by a factor λ to get a new domain \tilde{D} , the corresponding volumetric flow rate $w(\tilde{e}) = \lambda^2 w(e)$ and the corresponding edge length $l(\tilde{e}) = \lambda l(e)$. As a result, $M_{\alpha, \beta}(\tilde{G}) = \lambda^{2\alpha + \beta} M_{\alpha, \beta}(G)$ and the quantity

$$\frac{M_{\alpha, \beta}(G)}{|D|^{\alpha + \beta/2}} \quad (8)$$

is invariant under rescaling, where $|D|$ denotes the area of the domain D .

As a result, motivated by (7) and (8), for each placenta $P = (D, O)$ with a traced vascular structure G , we define the *shape factor* of G to be

$$S_{\alpha, \beta}(G) := \frac{\sum_{e \in E(G)} d(e)^{3\alpha} l(e)^\beta}{|D|^{\alpha + \beta/2}} \propto \frac{M_{\alpha, \beta}(G)}{|D|^{\alpha + \beta/2}}. \quad (9)$$

Also, we consider *transport efficiency* of G

$$E_{\alpha, \beta}(G) := \frac{\tilde{S}_{\alpha, \beta}}{S_{\alpha, \beta}(G)},$$

where $\tilde{S}_{\alpha, \beta}$ is a fixed constant. Here, we take it to be the mean of $S_{\alpha, \beta}(G)$ among all traced vascular structure G from the NCS group.

4.1. Comparison between NCS placentas and EARLI placentas via a family of transport cost functions

Let \mathcal{P}_N^a (and \mathcal{P}_N^v) denote the set of all traced arterial (and venous, respectively) vascular networks G from placentas in the NCS group, and \mathcal{P}_E^a (and \mathcal{P}_E^v) denote the set of all traced arterial (and venous, respectively) vascular networks G from placentas in the EARLI group.

Now, for each value α and β , by (9), we can calculate the shape factors $S_{\alpha,\beta}(G)$ for each G obtained from the above sets. Similarly, we can also calculate the transport efficiency $E_{\alpha,\beta}(G)$ for each G .

We claim that the values of these calculated transport efficiency $E_{\alpha,\beta}(G)$ can be used to distinguish the difference between the NCS group and the EARLI group, which in turn will give us indicators of the risk of an ASD diagnose.

To see it, we consider the *relative transport efficiency* functions of the two groups:

$$\begin{aligned} R^a(\alpha, \beta) &:= \frac{\text{mean}(\{S_{\alpha,\beta}(G) : G \in \mathcal{P}_N^a\})}{\text{mean}(\{S_{\alpha,\beta}(G) : G \in \mathcal{P}_E^a\})} \\ &= \frac{\text{mean}(\{E_{\alpha,\beta}(G) : G \in \mathcal{P}_N^a\})}{\text{mean}(\{E_{\alpha,\beta}(G) : G \in \mathcal{P}_E^a\})} \end{aligned}$$

for arteries and

$$\begin{aligned} R^v(\alpha, \beta) &:= \frac{\text{mean}(\{S_{\alpha,\beta}(G) : G \in \mathcal{P}_N^v\})}{\text{mean}(\{S_{\alpha,\beta}(G) : G \in \mathcal{P}_E^v\})} \\ &= \frac{\text{mean}(\{E_{\alpha,\beta}(G) : G \in \mathcal{P}_N^v\})}{\text{mean}(\{E_{\alpha,\beta}(G) : G \in \mathcal{P}_E^v\})} \end{aligned}$$

for veins. If \mathcal{P}_E^a (and \mathcal{P}_E^v) is a randomly selected subset of \mathcal{P}_N^a (and \mathcal{P}_N^v , respectively), one would expect that the values of $R^a(\alpha, \beta)$ (and $R^v(\alpha, \beta)$, respectively) are nearby one for any α and β .

Figure 5 and Figure 6 give us the plots of the curves $R^a(\alpha, \beta)$ and $R^v(\alpha, \beta)$ as a function of β for fixed values of α .

Based on Figure 5 and Figure 6, we have the following observations:

- \mathcal{P}_E^a (or \mathcal{P}_E^v) is not a randomly selected subset of \mathcal{P}_N^a (or \mathcal{P}_N^v respectively). The behaviors of traced vascular graphs of EARLI placentas are different from those of NCS placentas. These differences can be quantified by the relative transport efficiencies $R^a(\alpha, \beta)$ or $R^v(\alpha, \beta)$.
- The values of the relative transport efficiency $R^a(\alpha, \beta)$ and $R^v(\alpha, \beta)$ vary according to the transport cost function $x^\alpha y^\beta$. Under some transport costs, EARLI placentas are relatively more transport efficient than NCS placentas, while for other transport costs, the opposite situation appears.
- $R^a(\alpha, \beta)$ and $R^v(\alpha, \beta)$ are decreasing functions in both variables α and β .

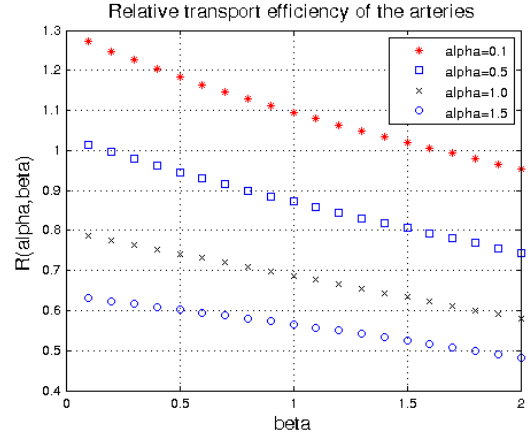


FIG. 5: Relative transport efficiency $R^a(\alpha, \beta)$ of arteries.

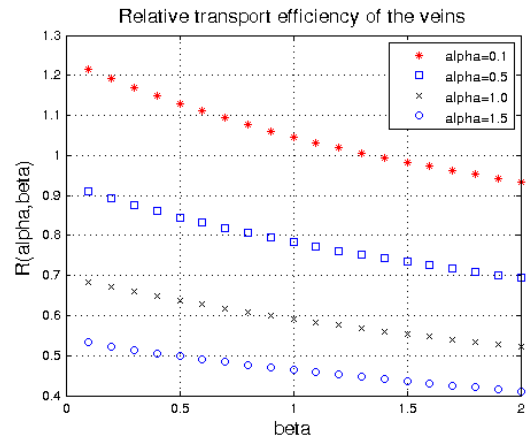


FIG. 6: Relative transport efficiency $R^v(\alpha, \beta)$ of veins.

- For each fixed α , $R^a(\alpha, \beta)$ and $R^v(\alpha, \beta)$ are nearly linear functions of β with negative slopes.

These observations demonstrate that there are significant differences between EARLI placentas and NCS placentas, in terms of these transport efficiency estimates.

4.2. Detailed comparison between NCS and EARLI placentas via the quadratic transport cost function

In this subsection, we will demonstrate that the calculated “transport efficiency” $E_{\alpha,\beta}(G)$ of the measured arterial/venous network G of a newborn’s placenta can be used as an indicator of the risk of a future ASD diagnosis. To illustrate this idea, here we consider a fixed transportation cost function, e.g. the quadratic transport cost $f(x, y) = xy^2$ with $\alpha = 1$ and $\beta = 2$. By Figure 5 and Figure 6, the values $R^a(1, 2) = 0.58$ and $R^v(1, 2) = 0.52$. These numbers says that in average, the arterial as well as

the venous network in an EARLI placenta is nearly half transport efficient when comparing with the one in an NCS placenta.

To better illustrate the difference of these two groups, we consider their corresponding probability density functions of transport efficiency $E_{1,2}(G)$ for both arterial and venous network in placentas of each group, and plot them together in Figure 7.

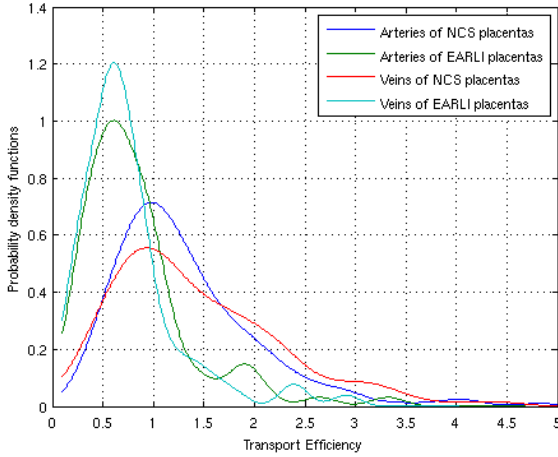


FIG. 7: Probability density functions of transport efficiency $E_{1,2}(G)$ derived from arterial/venous network G of NCS and EARLI placentas.

Similarly, we plot the graphs of their corresponding cumulative distribution functions of transport efficiency $E_{1,2}(G)$ in Figure 8. For example, from the graphs, we

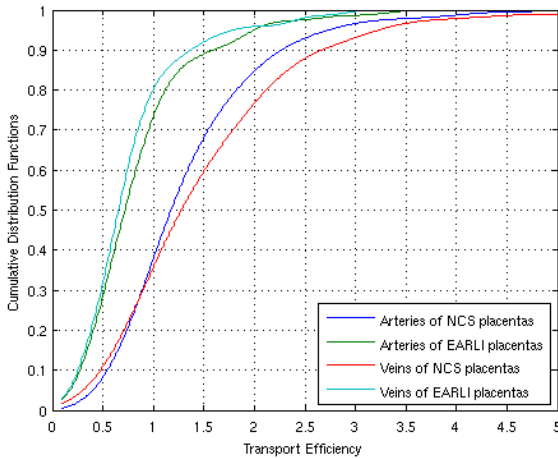


FIG. 8: Cumulative distribution functions of transport efficiency derived from arteries/veins of NCS and EARLI placentas.

see that in the NCS group, there are about 40% placentas whose transport efficiency of arteries is at most 1, and 35%

placentas whose transport efficiency of veins is at most 1. On the other hand, in the EARLI group, there are about 75% placentas whose transport efficiency of arteries is at most 1, and 80% placentas whose transport efficiency of veins is at most 1. These proportions in EARLI are approximately double those in NCS. Both Figure 7 and Figure 8 indicate again that arterial/venous networks from the EARLI placentas typically have much lower transport efficiency than those from the NCS placentas.

Figure 9 plots the ratio of the cumulative distribution function (CDF) of transport efficiency for both arterial and venous networks, respectively in the EARLI group over the CDF in the NCS group. In other words, when counting the total number of placentas whose arterial/venous network G having a transport efficiency $E_{1,2}(G)$ at most x , the number of such placentas in the EARLI group is $r_a(x)$ (or $r_v(x)$, respectively) multiples of those in the baseline i.e. the NCS group.

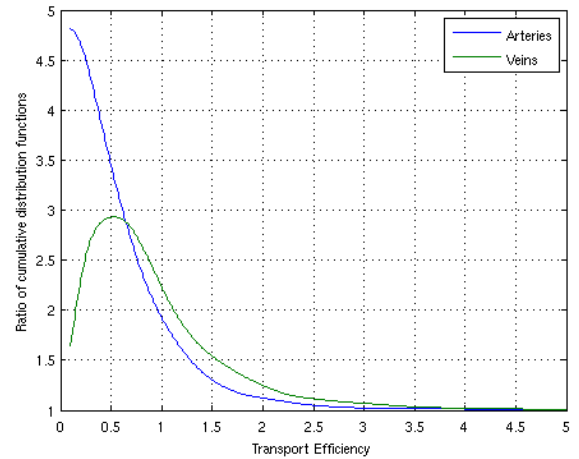


FIG. 9: Ratio of the cumulative distribution functions of transport efficiency derived from arterial/venous networks of EARLI placentas over the corresponding one of NCS placentas.

Note that the ratio $r_a(x)$ corresponding to arteries is a strictly decreasing function of transport efficiency, and is always greater than 1, suggesting that the relative probability of a placenta examined in this study belonging to the EARLI group vs. the NCS group decreases monotonically as arterial transport efficiency increases. For instance, when the transport efficiency x increases from $0.3 \rightarrow 0.5 \rightarrow 1 \rightarrow 1.5 \rightarrow 2$, the corresponding ratios $r_a(x)$ decrease rapidly from $4.5 \rightarrow 3.5 \rightarrow 1.8 \rightarrow 1.35 \rightarrow 1.2$.

The ratio function $r_v(x)$ corresponding to veins is still strictly decreasing, except for the region $x \in [0, 0.5]$ where transport efficiency is small. A possible explanation could be that when transport efficiency of veins in a placenta is too small, the fetus is no longer viable. This is supported by an earlier study in [25] which indicated that newborns with

very lower transport efficient network in placentas tend to have very small birth weights. Placentas from those non-surviving fetus were not included in the EARLI study.

4.3. Comparison between venous networks and arterial networks

For each placenta P with a venous network G_P^v and an arterial network G_P^a , we can calculate its corresponding shape factors $S_{\alpha,\beta}(G_P^v)$ and $S_{\alpha,\beta}(G_P^a)$ for each α and β , as indicated in Figure 10.

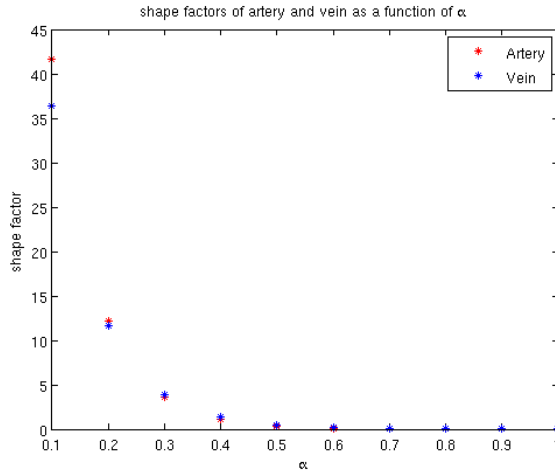


FIG. 10: The graphs of shape factors $S_{\alpha,\beta}(G_P^v)$ of the arterial network and $S_{\alpha,\beta}(G_P^a)$ of the venous network in a typical placenta with $\alpha \in [0, 1]$ and $\beta = 2$.

From Figure 10, one can see that both $S_{\alpha,\beta}(G_P^v)$ and $S_{\alpha,\beta}(G_P^a)$ are decreasing functions of α , but there is not much difference between the values of these two functions. This was the case for both NCS and EARLI placentas. An interesting phenomenon arises when we consider their ratios. Here, we define *the relative transport efficiency ratio* of veins over arteries by

$$R(\alpha, \beta, P) := \frac{S_{\alpha,\beta}(G_P^a)}{S_{\alpha,\beta}(G_P^v)} = \frac{E_{\alpha,\beta}(G_P^v)}{E_{\alpha,\beta}(G_P^a)}.$$

Fix $\beta = 2$. For each placenta P , we consider the function $R(\alpha) := R(\alpha, 2, P)$ as a function of $\alpha \in [0, 1]$, whose graph typically looks like a straight line as shown in Figure 11. When α is small and nearly 0, $R(\alpha) > 1$ indicating that the venous network is more transport efficient than the arterial network with respect to transport cost functions $f(x, y) = x^\alpha y^2$. When α becomes larger, $R(\alpha) < 1$ indicating that the venous network is less transport efficient than the arterial network with respect to transport cost functions $f(x, y) = x^\alpha y^2$.

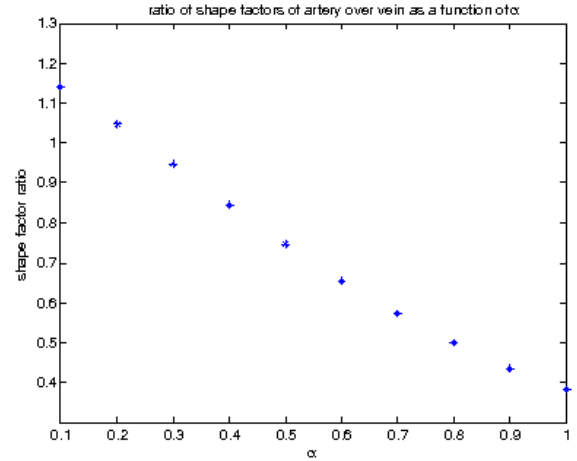


FIG. 11: The graph of $R(\alpha) = R(\alpha, 2, P)$ is typically a linear function of α for both NCS and EARLI placentas P .

Now, for each $\alpha \in [0, 1]$, we calculate the mean value of $R(\alpha) = R(\alpha, 2, P)$ among all placentas P in the NCS group, i.e. define

$$R_N(\alpha) := \text{mean}(\{R(\alpha, 2, P) : P \text{ in the NCS group}\}).$$

Similarly, for the EARLI group, we define

$$R_E(\alpha) := \text{mean}(\{R(\alpha, 2, P) : P \text{ in the EARLI group}\}).$$

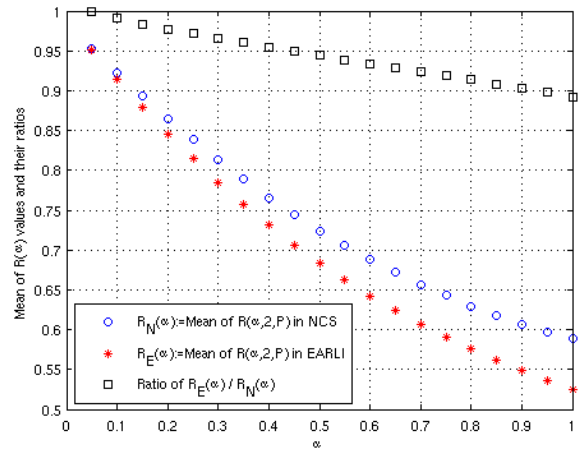


FIG. 12: Mean values of the relative transport efficiency ratio $R(\alpha, 2, P)$ of veins over arteries among placentas in either the NCS group or the EARLI group, and the ratio of mean values (EARLI/NCS).

In Figure 12, we plot the graphs of $R_N(\alpha)$, $R_E(\alpha)$, and their ratio $R_N(\alpha)/R_E(\alpha)$, as functions of $\alpha \in [0, 1]$.

Figure 12 indicates that both $R_E(\alpha)$ and $R_N(\alpha)$ are decreasing functions of α . Moreover, in general we have $R_E(\alpha) < R_N(\alpha)$. That is, placentas in the EARLI group tend to have smaller $R(\alpha)$ values than those in the NCS group. The largest difference is given when $\alpha = 1$.

Now, we want to view the value of the relative transport efficiency ratio $R(1) = R(1, 2, P)$ of veins over arteries as another approach to differentiating between the two groups. In Figure 13, we plot the probability density functions of $R(1) = R(1, 2, P)$ among all placentas P in the NCS group and also in the EARLI group. As shown in Fig-

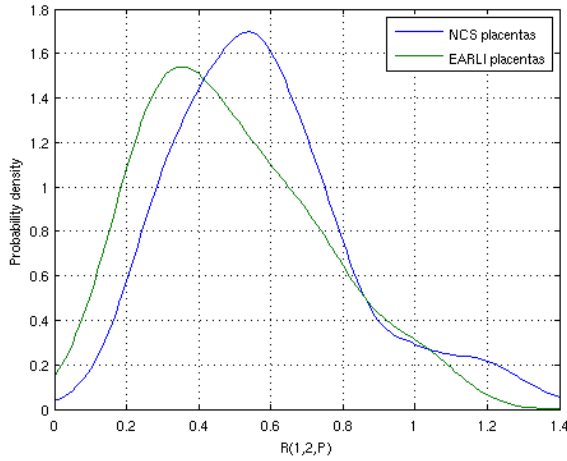


FIG. 13: Probability density of $R(1) = R(1, 2, P)$ among all P in the NCS group as well as in the EARLI group.

ure 13, placentas in the EARLI group tend to have smaller $R(1)$ values than those in the NCS group. The highest probability density of $R(1)$ values in the EARLI group is around 0.35, while the corresponding one in the NCS group is around 0.55. The difference between the NCS group and the EARLI group becomes even more clear when we consider the corresponding cumulative distribution functions of $R(1) = R(1, 2, P)$ among all placentas P in each group, as shown in Figure 14. For instance, there are about 25% NCS group placentas whose $R(1)$ values are no more than 0.4, while there are about 40% EARLI placentas whose $R(1)$ values are no more than 0.4. Both Figure 13 and Figure 14 demonstrate that there is a significant difference between $R(1)$ values in the EARLI group and those in the NCS group. The value of $R(1) = R(1, 2, P)$ is another potential discriminator of ASD risk.

In addition, the ratio of the cumulative distribution function of $R(1)$ from the EARLI group over those from the NCS group is shown in Figure 15. The lower the $R(1)$ value is, the higher probability of a placenta being in the EARLI group. As $R(1)$ increases, the ratio decreases rapidly especially for small $R(1)$ values. When $R(1)$ reaches approximately 0.6, the ratio becomes nearby 1, indicating that the

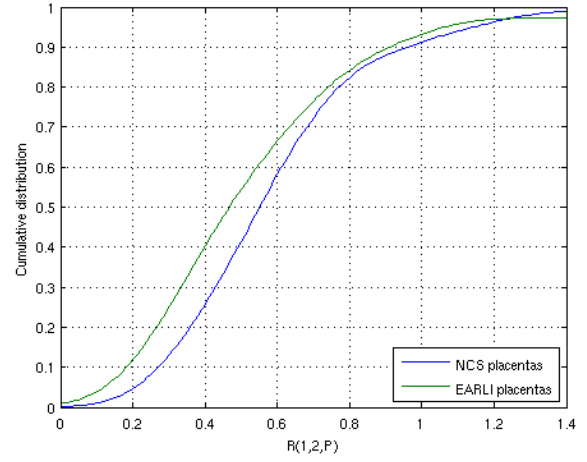


FIG. 14: The cumulative distribution functions of $R(1) = R(1, 2, P)$ among all P in the NCS group as well as those in the EARLI group.

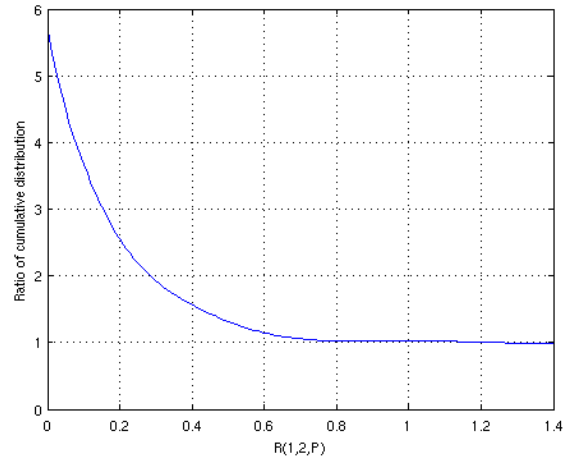


FIG. 15: The ratio of the cumulative distribution function of $R(1)$ from the EARLI group over those from the NCS group.

risk of an ASD diagnosis has declined to the level of the baseline.

Conclusions

Here, by studying the traced vascular structures inside (human) placentas via optimal transportation techniques, we identify two measurable anatomical indicators that appear to differentiate placentas from births to children with older siblings diagnosed with an ASD from a general sample of placentas. The first indicator is given in subsection 4.2 by the transport efficiency $E_{1,2}(G)$ of the measured venous/arterial network G of the placenta. Placentas

from children with older siblings diagnosed with an ASD had lower transport efficiency. Another indicator is given in subsection 4.3 by the relative transport efficiency ratio $R(1) = R(1, 2, P)$ of the venous network over the arterial network of the same placenta. The lower the relative transport efficiency ratio is, the greater the chance an examined placenta was from the EARLI sample. These results support further exploration of placental vascularization in etiologic mechanisms related to neurodevelopment. In addition, studies contrasting placental vascularization in births to children who go on to have an ASD diagnosis and those who do not, in both high risk (i.e., families where there is already a child diagnosed with ASD) and general population samples, should be completed to give a better indication of whether or not placental vascularization can be considered

further as a biomarker of ASD risk.

Acknowledgments

The work of Q. Xia is supported by NSF grant DMS-1109663. The work of C. M. Salafia is partially supported by NIH grant R01-HD39373-01 and SBIR grant 1 R43HD062307-01. The EARLI study was funded by R01ES016443 and Autism Speaks 9502. Some EARLI participants were recruited with the assistance of the Interactive Autism Network (IAN) database at the Kennedy Krieger.

-
- [1] American Psychiatric Association, Diagnostic and Statistical Manual of Mental Disorders, Fifth Edition, ISBN 978-0-89042-554-1.
- [2] Autism and Developmental Disabilities Monitoring Network Surveillance Year 2002 Principal Investigators, Centers for Disease Control and Prevention. Prevalence of autism spectrum disorders—autism and developmental disabilities monitoring network, 14 sites, United States, 2002. *MMWR Surveill Summ.* 2007 Feb 9;56(1):12-28.
- [3] D.J.P. Barker, Fetal origins of coronary heart disease. *BMJ* 311 (1995), 171-174.
- [4] M. Bernet; V. Caselles; J. Morel, Traffic plans. Optimal Transportation Networks: Models and Theory. Series: Lecture Notes in Mathematics, Vol. 1955, (2009).
- [5] A. Brancolini, G. Buttazzo, F. Santambrogio, Path functions over Wasserstein spaces. *J. Eur. Math. Soc.* Vol. 8, No.3 (2006),415–434.
- [6] D.L. Christensen, J. Baio J, K. Van Naarden Braun, D. Bilder, etc. Prevalence and Characteristics of Autism Spectrum Disorder Among Children Aged 8 Years—Autism and Developmental Disabilities Monitoring Network, 11 Sites, United States, 2012. *MMWR Surveill Summ.* 2016 Apr 1;65(3):1-23. doi: 10.15585/mmwr.ss6503a1.
- [7] C.M. Corsello. Early intervention in autism. *Infants and Young Children.* Vol 18, No.2, pp 74-85, (2005).
- [8] H. Gray. *Anatomy of the Human Body.* Philadelphia: Lea & Febiger, 1918.
- [9] M.M. Fraz, etc. Blood vessel segmentation methodologies in retinal images – A survey. *Computer Methods and Programs in Biomedicine.* Vol 108, Issue 1, pp 407–433 (2012)
- [10] J.S. Gill, C.M. Salafia, D. Grebenkov, D.D. Vvedensky. Modeling oxygen transport in human placental terminal villi. *J Theor Biol.* 2011 Dec 21;291:33-41;
- [11] F. Maddalena, S. Solimini and J.M. Morel. A variational model of irrigation patterns, *Interfaces and Free Boundaries,* Volume 5, Issue 4, (2003), pp. 391-416.
- [12] T.M. Mayhew. A stereological perspective on placental morphology in normal and complicated pregnancies. *J Anat.* 2009 Jul;215(1):77-90.
- [13] R.A. Molteni. Placental growth and fetal/placental weight (F/P) ratios throughout gestation—their relationship to patterns of fetal growth. *Semin Perinatol.* 1984 Apr;8(2):94-100.
- [14] The National Children’s Study 2014: An Assessment. Panel on the Design of the National Children’s Study and Implications for the Generalizability of Results; Committee on National Statistics; Division of Behavioral and Social Sciences and Education; Board on Children, Youth, and Families; National Research Council; Institute of Medicine; Duncan GJ, Kirkendall NJ, Citro CF, editors. Washington (DC): National Academies Press (US); 2014.
- [15] C.J. Newschaffer, L.A. Croen, M.D. Fallin, etc. Infant siblings and the investigation of autism risk factors. *J Neurodev Disord.* 2012 Apr; 4(1):7. doi:10.1186/1866-1955-4-7.
- [16] S. Ozonoff, GS Young, A. Carter, D. Messinger, etc. Recurrence risk for autism spectrum disorders: a Baby Siblings Research Consortium study. *Pediatrics.* 2011 Sep;128(3):e488-95. doi: 10.1542/peds.2010-2825.
- [17] S. J. Rogers. Brief Report: Early intervention in autism. *Journal of Autism and Developmental Disorder,* Vol. 26, No. 2, 1996.
- [18] C.M. Salafia, M Yampolsky, DP Misra, O Shlakhter, D Haas, B Eucker, Placental surface shape, function, and effects of maternal and fetal vascular pathology. *Thorp J. Placenta.* 2010 Nov; 31(11):958-8 .
- [19] S. Sandin, P. Lichtenstein, R. Kuja-Halkola, H. Larsson, C. M. Hultman, A. Reichenberg. The familial risk of autism. *JAMA.* 2014 May 7; 311(17):1770-7. doi: 10.1001/jama.2014.4144.
- [20] Q. Xia, Optimal paths related to transport problems. *Communications in Contemporary Mathematics.* Vol. 5, No. 2 (2003) 251-279.
- [21] Q. Xia, The formation of tree leaf. *ESAIM Control Optim. Calc. Var.* 13, No. 2, 359–377 (2007)
- [22] Q. Xia, An application of optimal transport paths to urban transport networks. *Discrete and Continuous Dynamical Systems, Supp.* (2005), 904-910.
- [23] Q. Xia, Numerical Simulation of Optimal Transport Paths.

- arXiv:0807.3723. *the Second International Conference on Computer Modeling and Simulation*. Vol. 1, 2010, 521-525.
- [24] Q. Xia, and D. Unger. Diffusion-limited aggregation driven by optimal transportation. *Fractals*, Vol. 18, No. 2, 2010, 247-253.
- [25] Q. Xia and C.M. Salafia. Transport efficiency of the human placenta. *Journal of Coupled Systems and Multiscale Dynamics*. 2, 1-8 (2014)
- [26] Q. Xia. Motivations, ideas and applications of ramified optimal transportation. *ESAIM: Mathematical Modelling and Numerical Analysis*. Volume 49, Number 6, November-December 2015. Special Issue - Optimal Transport. pp 1791 - 1832.
- [27] M. Yampolsky, C.M. Salafia, O. Shlakter. Probability distributions of placental morphological measurements and origins of variability of placental shapes. *Placenta*. 2013; 34(6):493-6.
- [28] R.K. Seong, C.M. Salafia, D. D. Vvedensky. Statistical topology of radial networks: a case study of tree leaves. *Philosophical Magazine*, 2011, 1-16, iFirst.
- [29] R.K. Seong, P. Getreuer, Y. Li, T. Girardi, C.M. Salafia, D. D. Vvedensky. Statistical Geometry and Topology of the Human Placenta. *Advances in Applied Mathematics, Modeling, and Computational Science Fields Institute Communications*, Volume 66, 2013, pp 187-208.
- [30] R.G. Shah, C.M. Salafia, T. Girardi, L. Conrad, K. Keaty, A. Bartleotc. Shape matching algorithm to validate the tracing protocol of placental chorionic surface vessel networks. *Placenta*. 2015 Aug; 36(8): 944-6.

Appendix: Some information on the data related to NCS and EARLI placentas

The group of NCS placentas are collected by Project 18 of the National Children's Study (NCS) [14]. NCS is a population cohort study of children in the United States and as such would be expected to experience the baseline ASD risk seen in the general U.S. population. Project 18 was a sub-

study designed to collect all placentas at specific sites in a defined time period for births in the NCS. The objective was to develop placental assessment and exposure methods that would be easy to replicate in a large multi-site cohort study (such as the larger NCS). Demographic and clinical characteristics of the sample for Project 18 were similar to births enrolled in the larger NCS cohort beyond Project 18.

The group of EARLI placentas are collected from The Early Autism Risk Longitudinal Investigation (EARLI) Study. The EARLI cohort is a network of research sites that enrolled and follows a group of mothers of children with autism at the start of another pregnancy and documenting the development of the newborn child (sibling of the autism case) through three years of age [15]. The EARLI Study is examining possible environmental risk factors for autism and studying whether there is any interplay between environmental factors and genetic susceptibility. Placentas from live born children were collected from mothers recruited at four sites: (a) Southeast Pennsylvania, by researchers from Drexel University, The Children's Hospital of Philadelphia and the University of Pennsylvania; (b) Northeast Maryland, by researchers from Johns Hopkins University and Kennedy Krieger Institute; (c) Northern California, UC Davis by researchers from University of California at Davis, and the M.I.N.D. Institute; (d) Northern California, Kaiser Permanente, by researchers from Kaiser Permanente Division of Research. Protocols were approved by the pertinent Institutional Review Boards. Placentas were fixed in formalin for one week and then weighed after removal of umbilical cord and membranes, photographed, scanned, sliced and tissue sampled, selected, and separated out for processing into histology slides. Data were extracted from the images by perimeter detection algorithms and variables calculated as described previously [18]. Only singleton births were included in our analysis and placentas were excluded if placenta morphology measures could not be obtained.